# Spatio-temporal control of femtosecond laser filamentation and white-light generation

N. Kaya, G. Kaya, J. Strohaber, A. Kolomenskii, and H. Schuessler

Citation: AIP Conference Proceedings **1815**, 030007 (2017); doi: 10.1063/1.4976355
View online: http://dx.doi.org/10.1063/1.4976355
View Table of Contents: http://aip.scitation.org/toc/apc/1815/1
Published by the American Institute of Physics

# Spatio-Temporal Control of Femtosecond Laser Filamentation and White-Light Generation

N. Kaya[1,2,3, a)], G. Kaya[1,4, b)], J. Strohaber[5], A. Kolomenskii[1], and H. Schuessler[1, 2]

[1]*Department of Physics, Texas A&M University, College Station, Texas 77843, USA.*
[2] *Science Program, Texas A&M University at Qatar, Doha 23874, Qatar.*
[3]*Department of Physics, Giresun University, Giresun 28200, Turkey.*
[4]*Technical Sciences of Vocational School, Canakkale Onsekiz Mart University, Canakkale 17020, Turkey.*
[5]*Department of Physics, Florida Agricultural and Mechanical University, Tallahassee, Florida 32307, USA.*

[a)]*Corresponding author: necati.kaya@qatar.tamu.edu*
[b)]*gamze@physics.tamu.edu*

**Abstract.** Several possibilities are investigated to control spatio-temporal characteristics of the femtosecond filamentation process and the resulting white-light generation. We controlled the development of self-focusing, and resulting locations of filaments producing white-light in water by changing the transverse spatial phase of an initial Gaussian beam with a computer generated holographic technique and a spatial light modulator. We studied intense femtosecond filamentation and propagation of femtosecond pulses with different transverse modes in water. The filament propagation length was found to increase with Bessel-Gaussian modes of the beams, when more lateral lobes were used, under the conditions of the same peak intensity, pulse duration, and size of the central peak of the incident beam. We also investigated variations of white-light generation when the delay between the two pulses was varied. With a decrease of the relative delay, an enhancement of white-light output was observed, which at near-zero delays was reverted to a suppression of white-light generation.

## INTRODUCTION

In recent studies, researchers have been trying to gain optimal control over laser-matter interaction to a desired outcome via manipulating different laser parameters, such as peak intensity [1], wavelength [2], pulse length [3], pulse shape [4], or carrier-envelope phase [5]. In the center of these efforts, there are strategies that provide extended nonlinear propagation under controlled conditions, as applied to filaments [6] or individual sources of white-light. This phenomenon has been the subject of active research motivated by various potential applications such as remote spectroscopy [7], generation of few-cycle optical pulses [8], and generation of THz radiation [9]. In this work we study possibilities to control spatial characteristics of the femtosecond filamentation process and the resulting white-light generation. By creating and employing the laser beams with modulated phase and amplitude, we studied the production and control of white-light generation and filamentation in transparent media. These research went in the following directions: (i) study of filament propagation length of femtosecond pulses with different transverse modes, (ii) white light generation control with crossing beams of femtosecond laser pulses.

## FILAMENT PROPAGATION LENGTH OF FEMTOSECOND PULSES WITH DIFFERENT TRANSVERSE MODES

The transverse modes of Gaussian beam (GB), Laguerre Gaussian beam (LGB) and Bessel Gaussian beam (BGB) are described respectively by the following distributions of the field amplitude in cylindrical polar coordinates: $E_{GB}(r,$

*Turkish Physical Society 32nd International Physics Congress (TPS32)*
AIP Conf. Proc. 1815, 030007-1–030007-4; doi: 10.1063/1.4976355
Published by AIP Publishing. 978-0-7354-1483-9/$30.00

$z$=0,$t$=0)= $E_o e^{-r^2/w_0^2}$ , $E_{LGB}(r, z=0,t=0)= E_o\left[1-2(\beta r)^2\right]e^{-(\beta r)^2}$ , and $E_{BGB}(r, z=0,t=0)= E_o J_o(\alpha r)e^{-(\gamma r)^2}$ , where $E_o$ is the peak amplitude, $w_o$ is the radius of the beam profile at the $1/e^2$ level of intensity, and $J_o$ is the zero order Bessel function. The constants $\alpha$ , $\beta$ and $\gamma$ are chosen in such a way as to make the FWHM of the central lobes of the different transverse modes equal.

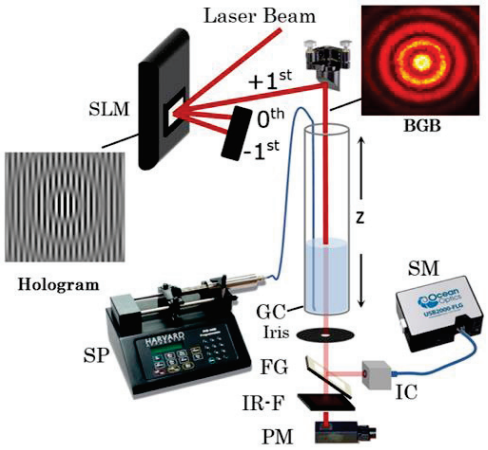


**FIGURE 1.** Experimental setup: SLM, spatial light modulator; SP, syringe pump; GC, glass cell with an optical window; FG, flat glass; IR-F or ND-F, infrared filter or neutral density filter; PM, power meter; IC, integrated cavity; SM, spectrometer. The inset under the SLM is an example hologram used to create a BGB with an intensity distribution illustrated in the top-right inset [10].

Laser modes were created from an initial GB of a Ti:sapphire laser system by using computer-generated holograms [11] displayed on a liquid crystal of a silicon spatial light modulator (Hamamatsu LCOS-SLM X10468-2). Figure 1 shows an illustration of the experimental setup used. The laser beam illuminates the SLM with a phase-amplitude encoded hologram set by a computer to produce a desired optical beam in the 1st diffraction order. Such grayscale computer-generated holograms for GB, LGB and BGB, prepared with a MATLAB code, were displayed on the SLM's LCD via a digital visual interface connection. An illustration of the computer-generated hologram used to produce a BGB in the first diffraction order is shown in the inset of Fig. 1.

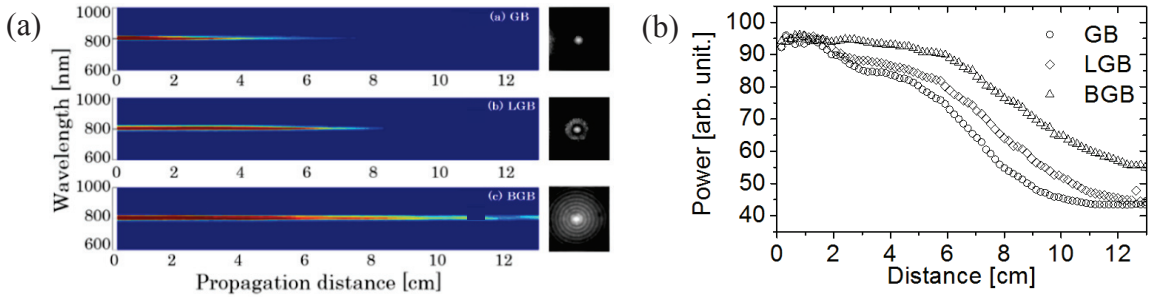


**FIGURE 2.** (a) Spectral profiles of the GB, LGB, and BGB measured over the central lobes as a function of the propagation distance. The corresponding experimentally created input beam modes are shown in the right panel. (b) IR power measured for GB, LGB, and BGB as a function of the propagation distance.

The filamentation phenomena occur with the resulting dynamic balance of self-focusing and plasma defocusing. For this reason, the sufficient peak power of $P_{in}$ =5.4 GW, which is much larger than the critical power for self-focusing in water, $P_{cr}$ =3.6MW, assured filament formation in the water cell. Indeed, hot spots in the beam producing white light corresponding to multiple filament formation were directly observed in our experiments. Figure 2 (a) shows spectra of the GB, LGB, and BGB, which were obtained by measuring over the central lobe of the beams, as a function of the propagation distance. The corresponding experimentally created beam modes are shown in the right panel of Fig. 2 (a). The self-focusing effect took place near the entrance of the beam into the cell (the self-focusing length was ~ 2cm), and the changes due to nonlinear effects in the spectral profiles of all three types of beams were observed

during subsequent propagation. The spectrum for the incident GB mode has the greatest depletion as the pulse propagates in the nonlinear medium followed by that of the incident LGB mode. The spectral profile of the incident BGB exhibits the least depletion among the three transverse modes as a function of distance. In Fig. 2 (b), we show the infrared power measured for only the central peak of the GB, LGB, and BGB as a function of the propagation distance. The trend of propagation distance elongation, similar to the one presented in Fig. 2(b), was recently demonstrated experimentally by using dressed beams, where the central Gaussian beam is surrounded by auxiliary dressing beam, which is wider and has a lower intensity [12]. Since a Bessel-like beam, which has an annular structure, possesses an inward energy flux towards its optical axis, it is expected to be well suited to replenish the filament core, as is confirmed by our measurements. Also, when we compare our results with recent theoretical studies on filamentation of femtosecond beams with different transverse modes in Ar gas [13], we see a similar effect that the central core in BGB mode is sustained for a longer propagation distance (compared to GB and LGB).

## WHITE LIGHT GENERATION CONTROL WITH CROSSING BEAMS OF FEMTOSECOND LASER PULSES

In the experiment on the white light generation control with crossing beams of femtosecond laser pulses (see Fig. 3), we used amplified femtosecond laser pulses (Spitfire, Spectra Physics) with 50 fs duration and initial energy up to 1 mJ at 1 kHz repetition rate. The pulses were focused by a curved mirror with a focal length of 2.5m, split into two sub-beams, and propagated in two optical arms with approximately equal optical paths. The optical path of one of the arms, labeled "movable arm" could be varied relative to the other arm, labeled "fixed arm" by a computer-controlled motorized translation stage (ESP301, Newport) with a temporal resolution of 0.33fs (0.00005mm). The two sub-beams crossed in the sample at an angle of 2.68 deg. The IR (around 800 nm) radiation and white light were separated by a dielectric mirror, effectively transmitting light from 400 to 600 nm and reflecting light at around 800 nm. We measured the power of the IR 800 nm radiation and that of white-light in the adjustable and fixed arms depending on the relative delay with an Ophir power meter. Alternatively, IR radiation and white light were imaged by projecting them onto a CCD camera.

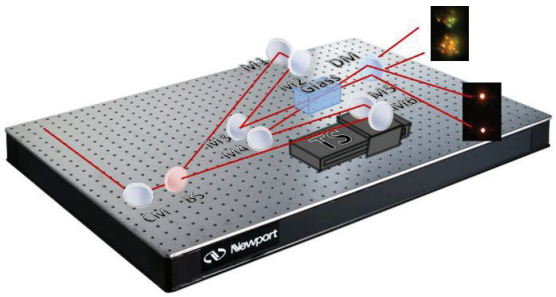


**FIGURE 3.** Experimental setup: the delay between pulses in two optical arms is changed by a translation stage. The two beams cross in a glass sample. Shown are: A- aperture, CM -curved mirror, BS - beam splitter, TS - translation stage, M1- M6 fast silver mirrors, DM - dielectric mirror.

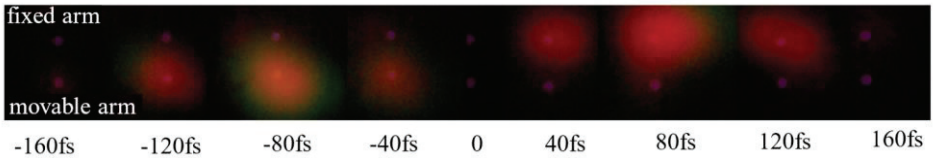


**FIGURE 4.** Images of beam cross-sections taken with 40 fs intervals of time delays.

Figure 4 shows a series of pictures of the cross-section of the beams taken for different delays with equal time intervals of 40 fs. In each picture the upper colored ones show light in the movable arm and the lower spot corresponds to the fixed arm. The power output of white light was measured in each of the arms by alternatively blocking half of the output plane; the total amount of white-light output produced in both arms was also measured. We define the delay time as the arrival time of the pulse in the fixed arm minus the arrival time of the pulse in the movable arm. When the delay was changed the amount of the generated white-light experienced variations in both arms (Fig. 5(a)). The power measured in the movable arm peaked at negative delays then dipped near zero delays even below the initial level and showed a minor peak at positive delays. The white-light output in the fixed arm qualitatively showed a behavior

reversed with respect to the delay time compared to the movable arm. Consequently, the amount of white light production increased for pulse that was lagging, and the total output of white-light of both arms exhibited two well pronounced peaks with a deep valley in between. Around zero delay the white light level goes to the level that is below the level found for large delays, when pulses do not overlap.

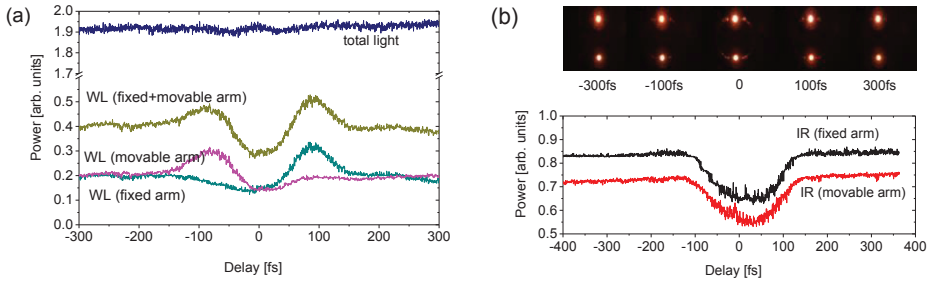


**FIGURE 5.** (a)Variations of the white-light (WL), total light and (b) infrared light (IR) (the upper diagram shows distributions in the cross sections of the beams: top –movable arm, bottom – fixed arm) vs. relative delay of two beams [10].

To explain the variations the generated white-light, we noticed a redistribution of the intensity in the cross-sections of the beams and, in addition, the measured power of the transmitted IR radiation through the sample revealed a suppression of the power in the central portion of the beams near zero delays (Fig. 5(b)). This means that some of the energy in the beams was deflected to the peripheral areas resulting in a well pronounced arc-shape extending from the central part of the beam. As a result, after the beams pass each other they experience a cylindrical lensing effect, leading to a local increase of intensity and enhanced filament formation. However, with a further decrease of the delay, the redistribution of the laser intensity due to formation of the lateral extensions becomes significant and results in the decrease of both the peak intensity in the central parts of the beams and the number of created filaments and, consequently, in a lower level of the generated white-light.

## ACKNOWLEDGMENTS

This work was supported by the Robert A. Welch Foundation Grant No. A1546 and the Qatar Foundation under the grant NPRP 6-465-1-091.

## REFERENCES

1. K. C. Kulander, F. H. Mies and K. J. Schafer, Phys. Rev. A **53**, 2562 (1996).
2. J. H. Posthumus, Rep. Prog. Phys. **67**, 623–665 (2004).
3. A. D. Bandrauk and H. Z. Lu, Phys. Rev. A **73** 013412 (2006).
4. M. Y. Shverdin, D. R. Walker, D. D. Yavuz, G. Y. Yin and S. E. Harris, Phys. Rev. Lett **94**, 033904 (2005).
5. G. G. Paulus, F. Grasbon, H. Walther, P. Villoresi, M. Nisoli, S. Stagira, E. Priori and S. D. Silvestri, Nature **414**, 182 (2001).
6. J. Bethge, C. Bree, H. Redlin, G. Stibenz, P. Staudt, G. Steinmeyer, A. Demircan and a. S. Duesterer, J. Opt. **13**, 055203 (2011).
7. Q. Luo, H. L. Xu, S. A. Hosseini, J. F. Daigle, F. Théberge, M. Sharifi and S. L. Chin, Appl. Phys. B **82**, 105-109 (2006).
8. C. P. Hauri, W. Kornelis, F. W. Helbing, A. Heinrich, A. Couairon, A. Mysyrowicz, J. Biegert and U. Keller, Appl. Phys. B **79**, 673-677 (2004).
9. C. D'Amico, A. Houard, M. Franco, B. Prade, A. Mysyrowicz, A. Couairon and V. T. Tikhonchuk, Phys. Rev. Lett. **98**, 235002 (2007).
10. N. Kaya, "Filamentation and White Light Generation with Spatially and Temporally Controlled Femtosecond Radiation," PhD thesis, Texas A&M University, 2014.
11. J. Strohaber, G. Kaya, N. Kaya, N. Hart, A. A. Kolomenskii, G. G. Paulus and H. A. Schuessler, Opt. Express **19**, 14321-14334 (2011).
12. M. Scheller, M. S. Mills, M. A. Miri, W. B. Cheng, J. V. Moloney, M. Kolesik, P. Polynkin and D. N. Christodoulides, Nat Photonics **8**, 297-301 (2014).
13. Z. Song and T. Nakajima, Opt. Express **18**, 12923-12938 (2010).